The Journal of Neuroscience, May 1, 2000, *20*(9):3282–3294

A Spatiotemporal Wave of Turnover and Functional Maturation of Olfactory Receptor Neurons in the Spiny Lobster *Panulirus argus*

Pascal Steullet, Holly S. Cate, and Charles D. Derby

Department of Biology and Center for Neural Communication and Computation, Georgia State University, Atlanta, Georgia 30303

Olfactory receptor neurons (ORNs) of crustaceans are housed in aesthetasc sensilla that are located on the lateral flagellum of the antennule. We used young adult spiny lobsters to examine turnover of aesthetascs and functional maturation of their ORNs after molting. The proliferation zone for new aesthetascs is located in the proximal part of the aesthetasc-bearing region and progressively moves along a distoproximal axis. Older aesthetascs are lost in the distal part of the aesthetasc-bearing region. As a result, an aesthetasc may be shed three to six molts after it differentiates. Taurine-like immunoreactivity is elevated in ORNs of aesthetascs that have yet to emerge on the cuticular surface and thereafter decreases gradually and asynchronously. ORNs from the distalmost-developing aesthetascs lose taurine-like immunoreactivity immediately before sensillar emergence, whereas ORNs from the most proximal and lateral new aesthetascs retain taurine-like immunoreactivity throughout the intermolt stage after sensillar emergence. Furthermore, taurine-like immunoreactivity is inversely correlated with odor responsiveness. These results suggest that taurine-like immunoreactivity reveals immature ORNs and that their functional maturation is not synchronized with molting and may not be completed until many weeks after sensillar emergence. Our data suggest successive spatiotemporal waves of birth, differentiation and functional maturation, and death of ORNs.

Key words: olfaction; olfactory receptor neuron; turnover; functional maturation; development; aesthetasc sensillum; taurine; agmatine; activity labeling; spiny lobster

Turnover of olfactory receptor neurons (ORNs) in adult animals is a remarkable phenomenon that distinguishes the olfactory system from many other sensory and neuronal tissues (Farbman, 1992). In vertebrates, there is a highly dynamic regulation of cellular turnover, including birth, functional maturation, and death (Mackay-Sim and Kittel, 1991a; Calof et al., 1996, 1998). Turnover also occurs in the olfactory systems of invertebrates, including snails (Chase and Rieling, 1986) and arthropods [crayfish (Sandeman and Sandeman, 1996); holometabolous insects during metamorphosis (Hildebrand, 1982; Riesgo-Escovar et al., 1992; Truman et al., 1993)].

Turnover of the arthropod olfactory system differs from that of vertebrates and gastropods because arthropods have compartmentalized peripheral olfactory systems, in which ORNs are packed into specialized cuticular structures called sensilla. Typically, turnover of ORNs occurs by the addition and loss of sensilla, because addition and loss of ORNs to existing sensilla have not been demonstrated in any arthropods (Keil, 1992). Turnover is particularly dramatic for arthropods that experience a metamorphosis, such as holometabolous insects and crustaceans. Addition of sensilla and their ORNs is common in arthropods that grow without undergoing drastic morphological changes, i.e., hemimetabolous insects (Chapman and Greenwood, 1986; Jander and Jander, 1994; Brézot et al., 1997), ticks (Hess and Vlimant, 1986), and postmetamorphic crustaceans (Spencer and Linberg, 1986; Mellon and Alones, 1993; Sandeman and Sandeman, 1996). Such increases in the number of sensilla are usually related to enlargement of the animal's body (Jander and Jander, 1994; Brézot et al., 1997). During nonmetamorphic growth in arthropods, turnover involving addition and loss of sensilla has been described on the cockroach antenna (Schafer and Sanchez, 1973) and on the lateral flagellum of the antennule of the crayfish *Cherax destructor* (Sandeman and Sandeman, 1996). Sandeman and Sandeman (1996) found that with each molt, new olfactory sensilla, called aesthetascs, were added to annuli at the proximal end of the aesthetasc region of the flagellum and the distalmost annuli bearing aesthetascs were sloughed or broken off. They did not determine when the ORNs of the new aesthetascs became functionally mature.

The aim of our study is to examine the turnover of aesthetascs and the maturation of their ORNs during molting in the spiny lobster *Panulirus argus*. Spiny lobsters live for decades, have indeterminate growth (Hartnoll, 1982), and can possess >1000 aesthetascs on the lateral flagellum. Each aesthetasc contains several hundred ORNs that include representatives of most ORN types, thus making the aesthetasc the functional unit in this olfactory organ (Steullet et al., 2000). Because environmental conditions and a lobster's needs can vary dramatically over its life span, this is a good model for studying the dynamics of turnover. Our results show that turnover of the aesthetascs and their ORNs occurs across much of the lateral flagellum at each molt. Addition and loss of aesthetascs take place in the proximal and the distal part of the lateral flagellum, respectively. Maturation of the new

Received Nov. 5, 1999; revised Feb. 10, 2000; accepted Feb. 11, 2000.

This study was supported by the National Institute on Deafness and Other Communication Disorders Grant DC00312 and The Georgia Research Alliance. We thank Lonny Anderson, Bill Gibbs, and the staff of the Keys Marine Laboratory for collecting and shipping lobsters; Vivian Ngo and Kevin Maskol for technical assistance; Lynn Milstead for the drawing of the antennule in Figure 1; Dr. Robert Simmons for assistance with the scanning electron microscope; Dr. W. C. Michel for valuable discussions and technical assistance; and Dr. Paul Harrison for many helpful discussions and comments on this manuscript.

Correspondence should be addressed to Dr. Pascal Steullet, Department of Biology, Georgia State University, P.O. Box 4010, Atlanta, GA 30302-4010. E-mail: biopes@panther.gsu.edu.

ORNs is slow, starting distally and spreading proximally and thus creating a spatiotemporal gradient of age and functional maturity of ORNs.

MATERIALS AND METHODS

Animals. Caribbean spiny lobsters (*P. argus*) were collected in the Florida Keys, shipped by air to Georgia State University, held in 800 l aquaria (20–25°C) containing recirculating, filtered, and aerated Instant Ocean (Aquarium Systems, Mentor, OH), and fed shrimp and squid. Preadult and young adult animals of 60–80 mm carapace length were used for this study.

The molt staging of spiny lobsters was performed according to the technique of Lyle and MacDonald (1983), which allows discrimination of the following stages: postmolt (stages A and B), intermolt (stage C), and premolt (stages D_0–D_4). According to Travis (1954), the duration of an entire molt cycle in *P. argus* of the size used in our study ranges from ~2 to 8 months, depending on the time of year and water temperature.

Localization and quantification of addition and loss of annuli and aesthetascs. To identify changes in the number of annuli and in the distribution and abundance of sensilla after molting, we used a method similar to that developed by Sandeman and Sandeman (1996). Premolt lobsters were held individually in 80 l aquaria until they molted, and then the lateral flagella from the shed cuticular exoskeleton (exuvium) and from the postmolt lobster were collected and fixed (see Solutions and chemicals). The exuvium conserves all external morphological structures of the premolt animal, including the setae. The numbers of aesthetascs and accompanying setae (see Fig. 1) on each annulus of the exuvia (premolt flagella) and their corresponding postmolt flagella were counted using a Zeiss Axioskop microscope (Jena, Germany) after having previously cut aesthetascs and guard hairs close to their bases with fine surgical scissors. This surgical procedure was necessary to improve visualization of each aesthetasc because the aesthetascs are densely packed in rows and surrounded by long guard hairs. Before aesthetascs on the postmolt flagella were cut, the average length of the aesthetascs on each annulus was measured. Some of the postmolt flagella were further processed for immunocytochemistry as described below.

Odor-dependent activity labeling. To investigate the functional maturation of ORNs of newly emerged aesthetascs, we used an odor-dependent activity-labeling technique that relies on the permeation of 1-amino-4-guanidinobutane (agmatine) through cation channels after odor stimulation (Marc, 1999a,b; Michel et al., 1999). This technique underestimates the total number of odor-activated ORNs, because it labels ORNs that have agmatine-permeable channels and that are highly excited (Michel et al., 1999). This technique thus allows labeling of ORNs that are best-tuned to and excited by the test odor but not those that are inhibited by the test odor (Steullet et al., 2000). Nonetheless, this is an effective technique for examining relative differences in odor sensitivity, such as that of ORNs of different developmental ages or in different antennular regions. Details about the agmatine odor-dependent activity-labeling technique are given elsewhere (Michel et al., 1999; Steullet et al., 2000). In brief, a lateral flagellum from either intermolt (stage C) or early premolt (stage D_0) lobsters was excised and secured in a stimulation chamber (Derby, 1995) such that the distal part of the flagellum bearing the aesthetascs rested in an olfactometer with a flow of modified artificial seawater (ASW; see Solutions and chemicals). The cut proximal part of the flagellum was placed in a separate bath containing lobster saline (see Solutions and chemicals) and was dissected to expose the antennular artery, which was cannulated and perfused with oxygenated lobster saline. Odor stimuli were injected for 5 sec every minute for 60 min into the modified ASW flowing over the flagellum using an electronically driven valve. Stimuli included 20 mM agmatine only (control) or 20 mM agmatine together with an odor (odors listed in Solutions and chemicals). After odor stimulation was completed, the modified ASW was superfused for another 5 min to remove any possible free agmatine before perfusing the antennular artery with fixative (see Solutions and chemicals). The flagellum was then removed from the chamber, cut into six equal parts, and further fixed for at least 2 d at room temperature. Pieces from the distal, medial, and proximal parts of the flagellum were sectioned and processed for immunocytochemistry as described below.

Immunocytochemistry. The goals of immunocytochemistry were the following: (1) to use an anti-taurine IgG antibody as a marker of the developmental stage of ORNs and to quantify taurine-like immunoreactivity (IR) in ORNs from aesthetascs of different regions of the flagellum throughout the molt cycle and (2) to label odor-activated ORNs using an anti-agmatine IgG antibody after exposure of flagella to odors and agmatine, a channel-permeant cation (see Odor-dependent activity labeling).

Flagella were taken at various stages of the molt cycle [from less than a day after a molt (stages A and B) to a day before the next molt (approximately stage D_4)], cut in small parts, and fixed (see Solutions and chemicals) for at least 2 d at room temperature. Pieces of fixed flagella were washed with 0.2 M PBS at pH 7.4, dehydrated via a graded series of ethanol and absolute acetone, and infiltrated and embedded with Pelco Eponate 12 resin (Ted Pella, Redding, CA). Transverse and occasionally horizontal sections (0.5 μm thick) from distal to proximal parts of the aesthetasc-bearing region and from annuli located just proximally to the aesthetasc region were taken using an ultramicrotome and diamond knife. Sets of a few 0.5-μm-thick serial sections were taken at increments of 10 μm. This procedure gave an adequate sampling of each cluster of ORN cell bodies associated with a single aesthetasc, because the average diameter of the ORN cell bodies is ~10 μm (Steullet et al., 2000). Therefore, each set of serial sections represents different ORN cell bodies. Sections were placed in wells of Teflon-coated spot slides, deplasticized, rinsed in absolute methanol and distilled water, dried, incubated for 24 hr with a primary antibody [either polyclonal anti-taurine IgG antibody (Signature Immunologics, Salt Lake City, UT) or polyclonal anti-agmatine IgG antibody (Chemicon, Temecula, CA)], followed for 1 hr with a secondary antibody, a nanogold-conjugated goat anti-rabbit antibody (Amersham, Arlington Heights, IL), and revealed by silver intensification [for details, see Steullet et al. (2000)]. When the same tissue was tested for immunoreactivity to both anti-taurine and anti-agmatine antibodies, serial sections were alternatively incubated with one of these antibodies. The anti-taurine IgG antibody does not cross-react with L-alanine, L- and D-aspartate, L-arginine, agmatine, L-cysteine, GABA, L-glutamate, glycine, reduced glutathione, L-glutamine, L-methionine, L-serine, and L-threonine but does with hypotaurine (R. E. Marc, personal communication). Therefore, taurine-like IR in developing ORNs might reveal the presence of taurine or hypotaurine. However, it probably indicates the presence of taurine, because taurine is typically found in much higher concentrations than is hypotaurine in the nervous system of many species (Perry and Hansen, 1973; Huxtable, 1992).

Quantification of agmatine- and taurine-like immunoreactivity. Images of the sections were captured using a Zeiss Axioskop microscope with a bright-field video camera attached to a video board in a personal computer and analyzed using ScionImagePC software (Scion Corporation, Frederick, MD). We quantified agmatine- and taurine-like IR in aesthetasc ORN cell bodies. Cell bodies of all ORNs associated with a single aesthetasc form a cell cluster in the lumen of the flagellum. Aesthetascs were classified into four categories based on their percentage of ORNs with taurine-like IR; the categories were ~0, <50, ≥50, and ~100%. For odor- and agmatine-exposed flagella, the number of agmatine-labeled ORNs (i.e., odor-responsive ORNs) associated with each aesthetasc was quantified as described in Steullet et al. (2000).

Scanning electron microscopy. Flagella were removed from the animal, cut in small pieces, fixed, washed with 0.2 M PBS, pH 7.4, and dehydrated via a graded series of ethanol and absolute acetone followed by immersion in dimethoxypropane. Pieces of the flagella were mounted onto a stub, vacuum dried, sputter coated with gold–palladium (Desk II sputter coater; Denton Vacuum, Moorestown, NJ), and examined using a Leica S420 scanning electron microscope (Cambridge, UK).

Solutions and chemicals. Odor stimuli were the single chemicals AMP, ammonium chloride (NH_4), L-cysteine, glycine, and L-proline and an artificial oyster mixture, which contains 33 compounds and mimics the composition of oyster extract (Carr and Derby, 1986). These odors were selected because they are present in the food of spiny lobsters and are effective stimuli (Carr, 1988; Derby, 2000; Steullet et al., 2000). All compounds used as odor stimuli and agmatine were 99% pure and were purchased from Sigma (St. Louis, MO), except homarine (a component of the artificial oyster mixture), which was obtained from Chemicals Procurement Laboratories (College Point, NY).

For odor-dependent activity labeling, artificial lobster saline was composed of (in mM): 458 NaCl, 13.4 KCl, 13.6 $CaCl_2$, 9.8 $MgCl_2$, 14.1 Na_2SO_4, 3 HEPES, 1.9 glucose, and 1.2 NaOH, with pH adjusted to 7.4. A modified ASW had a low concentration of Na^+ and Ca^{2+} (10% normal Na^+ and Ca^{2+}) to reduce competition between agmatine and both Na^+ and Ca^{2+} for entry in the ORNs through cation channels (Michel et al., 1999). The composition of this modified ASW was (in

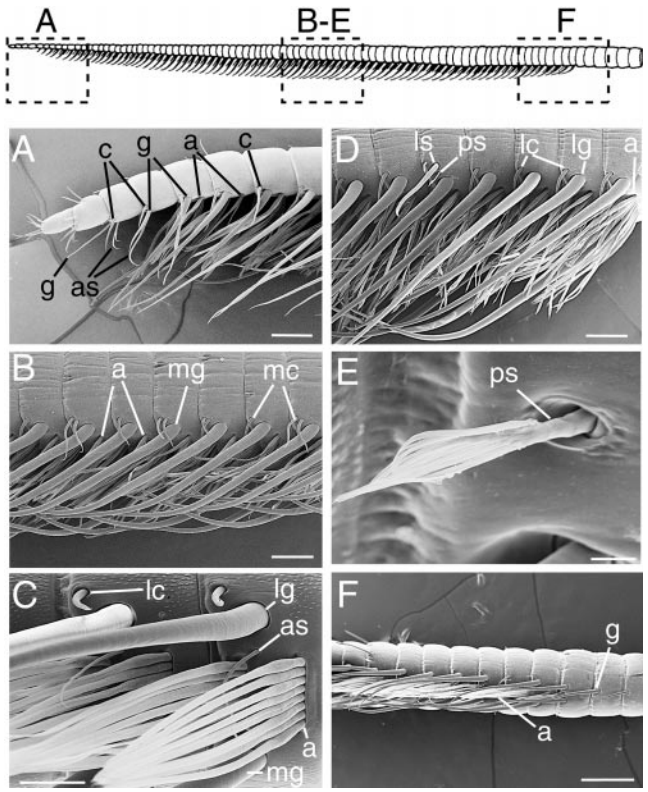

Figure 1. Lateral flagellum of the spiny lobster *P. argus*. *Drawing, Top,* The aesthetasc-bearing region that is located in the distal half of the lateral flagellum. *Letters A–F* indicate the relative position of the flagellar regions that are shown in each respective micrograph. *A*, Scanning electron micrograph showing the distal part of the flagellum. Note the absence of aesthetascs (*a*), normal-sized guard hairs (*g*), asymmetric hairs (*as*), and companion hairs (*c*) on the four most distal annuli. *B*, Scanning electron micrograph showing a mesial view of the flagellum with the aesthetascs (*a*) and their accompanying sensilla, including mesial companion hairs (*mc*) and mesial guard hairs (*mg*). Note the presence of one to two mesial companion hairs per annulus. *C*, Scanning electron micrograph showing a high-magnification view of rows of aesthetascs (*a*), asymmetric hairs (*as*), mesial and lateral guard hairs (*mg* and *lg*, respectively), and lateral companion hairs (*lc*). *D*, Scanning electron micrograph showing a lateral view of the flagellum with the aesthetascs (*a*) and their accompanying sensilla, including lateral companion hairs (*lc*), lateral guard hairs (*lg*), a long lateral seta (*ls*), and a plumose seta (*ps*). *E*, Scanning electron micrograph showing a high-magnification view of the plumose seta (*ps*) that usually replaces the lateral companion hair on an annulus that possesses a long lateral seta. *F*, Scanning electron micrograph of the proximal end of the aesthetasc region. Note the small number of aesthetascs (*a*) on the most proximal row and the presence of guard hairs (*g*) on the two annuli just proximal to the aesthetasc-bearing annuli. Scale bars: *A, B, D*, 200 μm; *C*, 100 μm; *E*, 20 μm; *F*, 400 μm.

mM): 42 NaCl, 412 *N*-methyl-D-glucamine·HCl, 9 KCl, 1 $CaCl_2$, 23 $MgCl_2$, 26 $MgSO_4$, and 2 $NaHCO_3$, pH 7.2.

The fixative used throughout our study was 2.5% glutaraldehyde, 1% paraformaldehyde, and 10% sucrose in 0.2 M PBS at pH 7.4.

RESULTS

Organization and distribution of aesthetascs and their set of accompanying sensilla

The lateral flagellum of the antennule, which is composed of segments called annuli, has a very stereotyped organization and distribution of sensilla (Fig. 1). Aesthetascs and their accompanying sensilla are restricted to the ventral side of annuli in the distal half of the lateral flagellum. On the 60- to 80-mm-carapace-length lobsters that we examined, an average of ~50% of the annuli (80 of 158) had aesthetascs, and the total number of aesthetascs per flagellum averaged 1330.

In general, each annulus in the aesthetasc-bearing region of the flagellum possesses a similar complement of setae and sensilla. Most of these setal types have been identified and named previously (Laverack, 1964; Gleeson et al., 1993). Each annulus has the following setae: two rows of aesthetascs (Fig. 1*C, a*); a pair of guard hairs that border the aesthetasc rows on the mesial (*mg*) and lateral (*lg*) margins, respectively (Fig. 1*C*); up to two companion hairs near the base of the mesial guard hair (Fig. 1*B,* mesial companion hair, or *mc*); one companion hair near the base of the lateral guard hair (Fig. 1*D,* lateral companion hair, or *lc*); and one asymmetric hair (Fig. 1*C, as*) whose base inserts just lateral to the aesthetasc rows and whose shaft extends mesially between the two rows of aesthetascs of an annulus. Occasionally, a previously undescribed simple seta (Lavalli and Factor, 1995), which we name the "long lateral seta" (Fig. 1*D, ls*), is present on the lateral side of an aesthetasc-bearing annulus. On such annuli, the asymmetric hair is absent, and the lateral companion hair is usually replaced by a previously undescribed "plumose seta" [Fig. 1*D,E, ps*; using the terminology of Watling (1989) and Lavalli and Factor (1995)]. In addition to the setae described above, other types of setae are present on the lateral and dorsal surfaces of the antennular annuli. However, a description of the distribution and organization of these setae is beyond the scope of the present paper.

Changes in antennular morphology and composition of sensilla after a molt

To follow changes in the number of antennular annuli and in setal distribution that occur at molting, we used a method similar to that of Sandeman and Sandeman (1996) to compare a freshly molted flagellum with its corresponding exuvium (i.e., premolt flagellum). This comparison was possible because of the unique and specific distribution of mesial companion hairs (Fig. 1*B, mc*) and long lateral setae (Fig. 1*D, ls*), which is generally retained after molting. This allowed us to align a given exuvium with its corresponding postmolt flagellum and to identify changes that occurred at molting on any particular annulus. As illustrated in Figure 2, the pattern of mesial companion hairs was very similar along the aesthetasc-bearing region of the exuvium and its corresponding region on the freshly molted flagellum. After a molt, only a few mesial companion hairs were added in the proximal region (Fig. 2, *black boxes* in *column mc*), and a few were lost on the most distal annuli (Fig. 2, *gray boxes* in *column mc*). Similarly, the pattern of long lateral setae could be matched along the aesthetasc-bearing region (Fig. 2, *column ls*). Importantly, the presence of long lateral setae on only a few annuli along the entire length of the flagellum allowed us to identify and quantify any net changes in the number of annuli between consecutive setae after a molt. For instance in Figure 2, it was apparent that annuli were added proximally but not distally to the aesthetasc-bearing region of the premolt flagellum. Changes in the number of annuli, aesthetascs, and other sensilla associated with the aesthetasc-bearing region of the flagellum that occur at a molt are described below.

Addition and loss of annuli

After molting, animals in our study had a 5.5 mm average increase in carapace length and an average addition of 10 annuli to their lateral flagellum. This represents an 8% increase in carapace length and a 7% increase in the number of annuli. Figure 3 shows

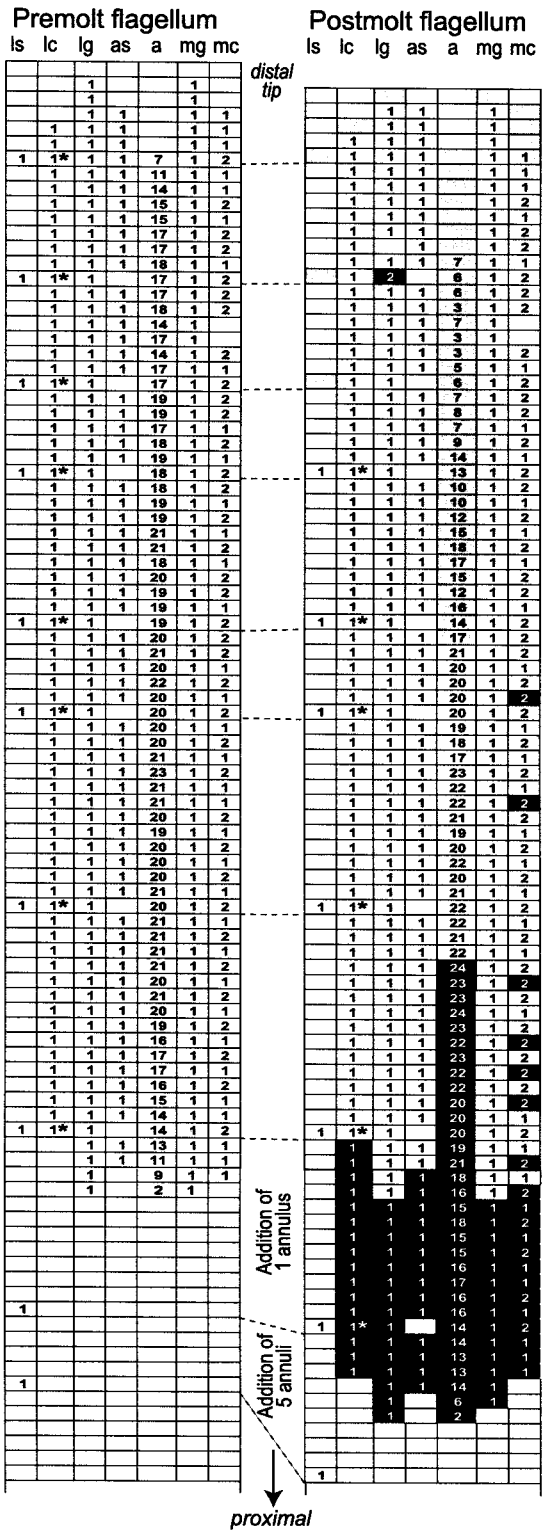

Figure 2. Example of the distribution of sensilla in the aesthetasc region on the premolt flagellum (exuvium; *left*) and its corresponding postmolt flagellum (*right*). Most of the proximal nonaesthetasc region is not shown. Each *row* corresponds to an annulus of the flagellum. Premolt and postmolt flagella are aligned so that patterns of distribution of the mesial companion hairs (*column mc*) and long lateral setae (*column ls*) are matching. Note the good matching of the pattern of the mesial companion hairs (*column mc*) in both premolt and postmolt flagella, with a few exceptions indicated in the postmolt flagellum as *gray boxes* for loss of sensilla and *black boxes* for gain of sensilla. Note that the distribution of the long lateral setae (*column ls*) is identical in the aesthetasc region of the premolt flagellum and its corresponding region on the postmolt flagellum, with the exception of the three most distal long lateral setae and associated plumose setae that disappeared after the molt (indicated as *gray boxes*). Note that proximal to the aesthetasc region of the premolt flagella, the position of the long lateral setae does not match with the position of the long lateral setae on the postmolt flagellum. This is caused by the addition of annuli between two consecutive setae. * indicates that the lateral companion hair was replaced by a plumose seta (Fig. 1*D,E, ps*). *a*, Aesthetascs; *as*, asymmetric hairs; *lc*, lateral companion hairs; *lg*, lateral guard hairs; *mg*, mesial guard hairs.

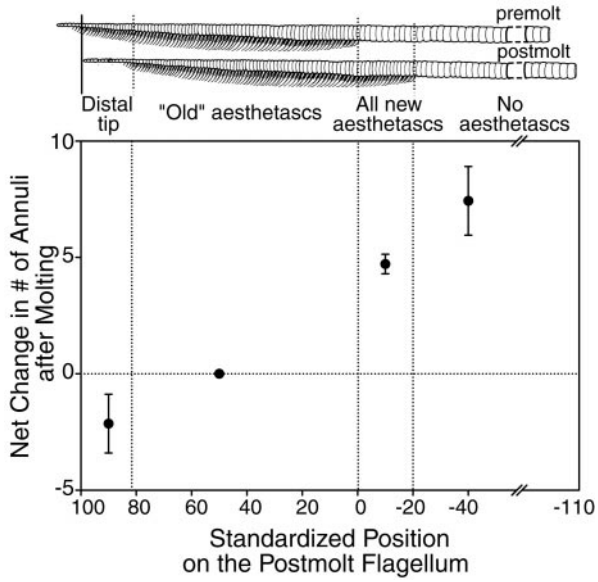

Figure 3. Net changes in the number of annuli in different parts of the lateral flagellum after molting. Values are means ± SEM, for seven flagella from four animals. Data are based on changes in the number of annuli between consecutive long lateral setae in different parts of the flagellum. These parts are the following: *Distal tip*, region at the tip with no or few aesthetasc-bearing annuli; *"Old" aesthetascs*, region of annuli with existing rows of aesthetascs; *All new aesthetascs*, region of annuli with newly emerged aesthetascs; and *No aesthetascs*, region of annuli without aesthetascs. For the nonaesthetasc-bearing region, the net change is based on the change in the number of annuli between the most distal long lateral setae along this region and the flagellar base. To quantify and compare changes in annuli after the molt on many different flagella of variable lengths, we standardized the length of each postmolt flagellum by using as fixed reference points the tip of the flagellum (*point* 100) and the most proximal annuli with 1-molt-cycle-old aesthetascs (*point* 0). *Negative numbers* along the standardized flagella indicate regions with annuli that did not bear aesthetascs before the last molt. To illustrate these regions and their standardized positions, *drawings* (*top*) of an exuvium (i.e., premolt flagellum) and its corresponding postmolt flagellum are shown such that an annulus on the exuvium is aligned with its corresponding annulus on the postmolt flagellum. *Breaks* in the *drawings* of the premolt and postmolt flagella and on the *x*-axis indicate that not all of the proximal nonaesthetasc-bearing annuli are shown in this figure.

the average net change in the number of annuli that occurred along different regions of the flagellum after molting. At the distal tip of the flagellum, there was usually a small net loss of annuli (Fig. 3). The flagellum illustrated in Figure 2, for example, lost two annuli at its distal tip after molting. However in one of the seven flagella examined, a net addition of two small annuli without aesthetascs was observed at the tip of the flagellum. The distal part of the aesthetasc-bearing region of this flagellum had been broken before the molt, which suggests that the net addition of

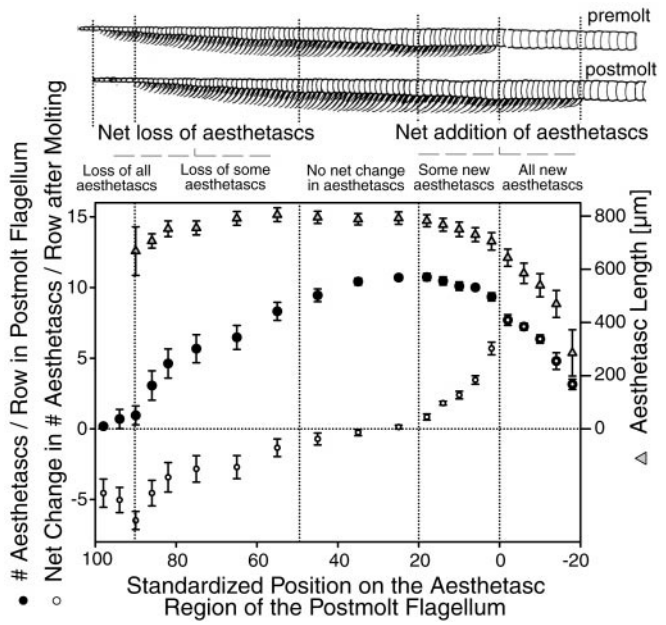

Figure 4. The number of aesthetascs per row (*filled circles*), the aesthetasc length (*open triangles*), and net changes in the number of aesthetascs per row (*open circles*) along different parts of the lateral flagellum after molting. Values are means ± SEM, for 10 flagella from six animals. To analyze and compare flagella of variable lengths, we standardized the length of each postmolt flagellum as described in Figure 3. *Drawings* (*top*) of a premolt and postmolt flagellum are shown such that an annulus on the premolt flagellum (i.e., exuvium) is aligned with its corresponding annulus on the postmolt flagellum.

distal annuli reflects regeneration, a process known to occur in the antennules and other appendages of these animals (Skinner, 1985). There was no net addition or loss of annuli in the aesthetascs-bearing region of the premolt flagellum (Fig. 3, *region* of *"Old" aesthetascs*). By contrast, the net addition of annuli occurred in the part of the flagellum that acquired new rows of aesthetascs (Fig. 3, *region* of *All new aesthetascs*) and in the proximal region where no rows of aesthetascs emerged at the molt (Fig. 3, *region* of *No aesthetascs*). This clearly indicates that division or addition of annuli takes place proximal to the aesthetasc-bearing region but not within the aesthetasc-bearing region. In the nonaesthetasc region of the flagellum, the annuli were more variable in length and on average longer than those in the aesthetasc-bearing region (see Fig. 3, schematic *drawings* of flagella). From this observation, we infer that there was addition of annuli proximal to the aesthetasc-bearing region and that annuli acquiring new aesthetascs underwent division, thereby being reduced in length. In the seven flagella examined, an average of 70% of the annuli that acquired new aesthetascs resulted from annular division. On the other hand, an average of only 22% of the annuli in the nonaesthetasc part of the flagellum (i.e., annuli that did not acquire aesthetascs after a molt) resulted from annular division or addition.

Addition and loss of aesthetascs

Aesthetascs were added proximally and lost distally from the aesthetasc-bearing region, and there was no change in the medial region. The pattern of net addition and loss that occurred at molting is illustrated in Figure 4. On average, 14 annuli acquired new rows of aesthetascs. These annuli were located immediately proximal to the aesthetasc-bearing region of the premolt flagellum (Fig. 4, *region 0 to −20*). There was a gradual decrease in both the number of aesthetascs per row and the length of aesthetascs within a row, from the most distal to the most proximal of these 14 annuli (Fig. 4). For example, the most distal annulus of this group (Fig. 4, *region just <0*) added two rows of approximately eight aesthetascs, whereas the most proximal ones (e.g., Fig. 4, *region just more than −20*) added rows with only a few short aesthetascs (Fig. 4). The most proximal annulus of this group acquired only a single row of two to three very short aesthetascs (see example in Fig. 2). The 14 most proximal aesthetasc-bearing annuli of the premolt flagellum (Fig. 4, *region 0–20*) had incomplete aesthetasc rows that had emerged at the previous molt. After molting, new aesthetascs were added to these rows such that the number of aesthetascs per row reached an average of 10. For example, the most distal annuli of this group (e.g., Fig. 4, *region just <20*) acquired only approximately one new aesthetasc on existing rows, whereas the most proximal ones (e.g., Fig. 4, *region just >0*) added an average of five new aesthetascs per row. We infer from these results that incomplete aesthetasc rows are added to annuli that had no aesthetascs previously and that these annuli will receive their full complement of aesthetascs (i.e., 10) after the following molt. In the medial part of the aesthetasc-bearing region (Fig. 4, *region ~20–50*), there was no net change in the number of aesthetascs per row after molting. Each annulus of this part of the flagellum possessed two rows of ~10 aesthetascs of similar length (Fig. 4). The number of aesthetascs per annulus decreased in the more distal part of the aesthetasc-bearing region (Fig. 4, *region ~50–85*). Thus in the most distal aesthetasc-bearing annuli (Fig. 4, *region 80–85*), rows housed an average of only three to five aesthetascs. This was caused by a gradual loss of aesthetascs after molting, this loss being greatest in the more distal annuli. Finally, on average, the 10 most distal aesthetasc-bearing annuli (Fig. 4, *region ~85–100*) lost their entire set of aesthetascs after molting.

Overall, there was an average net addition of three aesthetasc-bearing annuli after molting. This corresponded to a 4% increase in the number of annuli bearing aesthetascs. There was a median 1.4% increase in the total number of aesthetascs; this number increased in seven flagella (+6 to +125 aesthetascs) but decreased in three (−9 to −301 aesthetascs). Interestingly, the most dramatic loss of aesthetascs occurred in the two longest premolt flagella, and this was caused by a massive loss of aesthetascs along most of the distal half of the aesthetasc-bearing region. However in one flagellum (not included in the analysis) that was broken off at the medial part of the aesthetasc-bearing region, the total number of aesthetascs dramatically increased at a molt (+344 aesthetascs), suggesting an upregulation of the number of aesthetascs caused by damage.

Addition and loss of other sensilla in the aesthetasc region

Other sensilla, including guard, companion, and asymmetric hairs, followed closely the same pattern of turnover as did aesthetascs. Addition of these sensilla generally occurred on the same annuli that acquired new rows of aesthetascs. However, new guard hairs were often present on one to two annuli proximal to the most proximal row of aesthetascs (Fig. 1*F*). By contrast, companion hairs were typically absent on the most proximal annuli containing new rows of aesthetascs (Fig. 2). Addition of a few mesial companion hairs also occurred occasionally along the proximal part of the aesthetasc region where aesthetascs were added to existing rows (Fig. 2). In the distal end of the flagellum, guard, companion, and asymmetric hairs seemed to remain

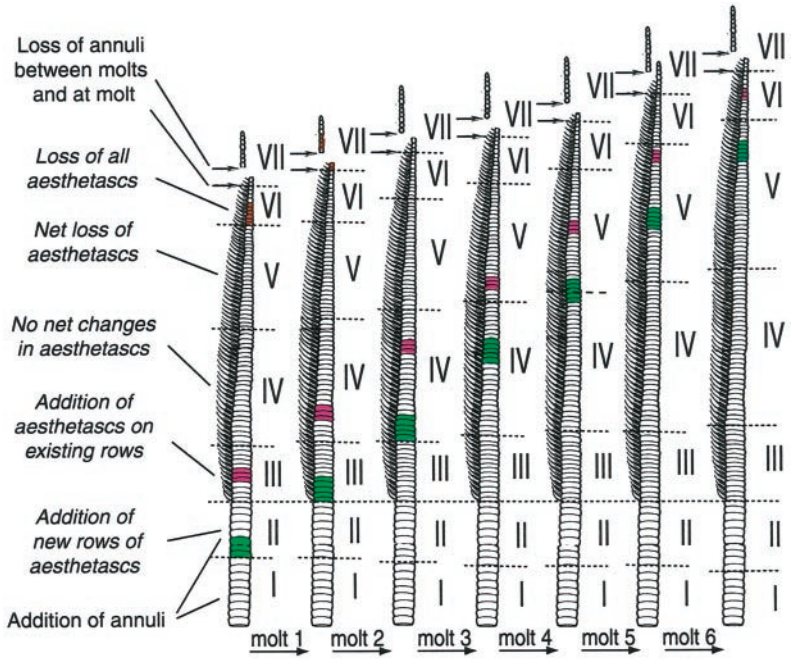

Figure 5. Drawings of a flagellum showing the turnover of aesthetasc-bearing annuli and the relative position of representative sets of annuli over a period of six molts. A few sets of annuli along the flagellum are *colored* to illustrate the relative movement of annuli toward the distal part of the flagellum as new rows of aesthetascs are developing and emerging on the cuticular surface of the proximal region and as the distal aesthetasc-bearing annuli are gradually losing their aesthetascs and are finally shed. *Regions* numbered from *I* to *VII* represent zones of the flagellum where distinct turnover-related events occur: *zone I*, addition of annuli; *zone II,* addition of annuli (indicated as an increase in the number of *green* annuli) and new rows of aesthetascs; *zone III*, addition of a few aesthetascs on existing rows of aesthetascs; *zone IV,* no net change in aesthetasc numbers; *zone V,* net loss of aesthetascs; *zone VI,* loss of all aesthetascs; and *zone VII,* no aesthetascs, with shedding of annuli between molts, presumably by damage, and at molting. This figure is based on the extrapolation over six molts of the data presented in the Results and Figures 3 and 4. It assumes that a given zone occupies the same proportion of the flagellar length over a period of six molts.

present almost up to the most distal annuli but decreased in size on annuli that lost all aesthetascs (Fig. 1*A*). Finally in a few cases, the most distal long lateral setae also disappeared after molting together with the plumose setae associated with them (Fig. 2).

Turnover and life span of aesthetasc-bearing annuli and aesthetascs

Turnover of aesthetascs occurs in a linear and orderly manner, and it is possible to distinguish seven zones on the basis of molt-related changes in the turnover of annuli and aesthetascs. These zones are depicted in Figure 5. Starting at the proximal base of the flagellum, zone I includes annuli that do not have and will not acquire aesthetascs after the next molt. In zone I, there is addition of annuli. Zone II includes annuli that do not bear aesthetascs but will acquire "incomplete" rows of aesthetascs after the next molt. In zone II, there is also addition of annuli. Zone III includes annuli with incomplete rows of aesthetascs. After molting, aesthetascs are added to these annuli such that they eventually will house complete rows (i.e., 10 aesthetascs per row). Zone IV includes annuli that have complete rows of aesthetascs. On these annuli, there is no net change in the number of aesthetascs after molting. Zone V includes annuli that have a full or less full complement of aesthetascs, but all will lose some aesthetascs at the next molt. After molting, therefore, the number of aesthetascs per row on these annuli will be reduced. Zone VI includes annuli that contain a reduced number of aesthetascs and will lose all of their remaining aesthetascs at the next molt. Zone VII includes the distal annuli that do not bear aesthetascs and that are dramatically smaller. Immediately after a molt, zone VII is quite long, but many of these annuli will be shed, presumably by damage, before the next molt. Finally, most of the remaining annuli of zone VII will be lost at the following molt.

As a result of the continual addition of new rows of aesthetascs on proximal annuli and the shedding of distal annuli, the relative position of each aesthetasc-bearing annulus shifts further distally along the flagellum at each molt. On the basis of an extrapolation from data on changes after a single molt, an annulus will shift from zone III (where new rows of aesthetasc emerge at the cuticular surface) to zone VI (where rows of old aesthetascs are shed) in approximately six molt cycles (Fig. 5). The life span of any particular aesthetasc, however, might be shorter because an annulus acquires aesthetascs during two molt cycles and gradually loses its aesthetascs through approximately three molts (Fig. 5).

Development of aesthetascs and their ORNs under the cuticle

The emergence of new aesthetascs after a molt was preceded by their development under the cuticle before molting. Transverse and horizontal sections of the lateral flagellum allowed the identification of the cell body clusters of ORNs and supporting cells associated with emerged aesthetascs (Fig. 6*A*) and the cell clusters associated with developing aesthetascs yet to emerge at the next molt (Fig. 6*B,C*). As described by Grünert and Ache (1988), each emerged aesthetasc was innervated by the outer dendrites of a few hundred ORNs, whose cell bodies were grouped in a cluster beneath the sensillum. Supporting cells enveloped the ORN inner dendrites that connect the ORN cell bodies to the outer dendrites in the sensillar shaft. Sections through zones II and III of flagella at different molt stages revealed where and approximately when developing aesthetascs yet to emerge at the next molt formed. The development of new aesthetascs was first indicated by the presence of clusters of cells protruding from the epidermis. Developing ORNs in these clusters initiated dendritic and axonal outgrowth. During the premolt stage, the cuticle formed around the dendrites of the developing ORNs to make the sensillum that emerged after the shedding of the old cuticle at molt. In zone II, where new rows of aesthetascs developed, only the most distal annuli contained developing clusters at postmolt and early intermolt stages; developing clusters appeared progressively in more proximal annuli during the intermolt and presumably part of the premolt stage. In zone III, developing clusters formed on the lateral side of clusters associated with existing aesthetascs (Fig. 6*B,C*); they were rarely observed in postmolt flagella (an average of 0.3 per annulus) but were frequent in intermolt flagella (an average of 2.8 per annulus; see Fig. 6*B,C*). Although the vast majority of the developing aesthetascs emerged at the next molt,

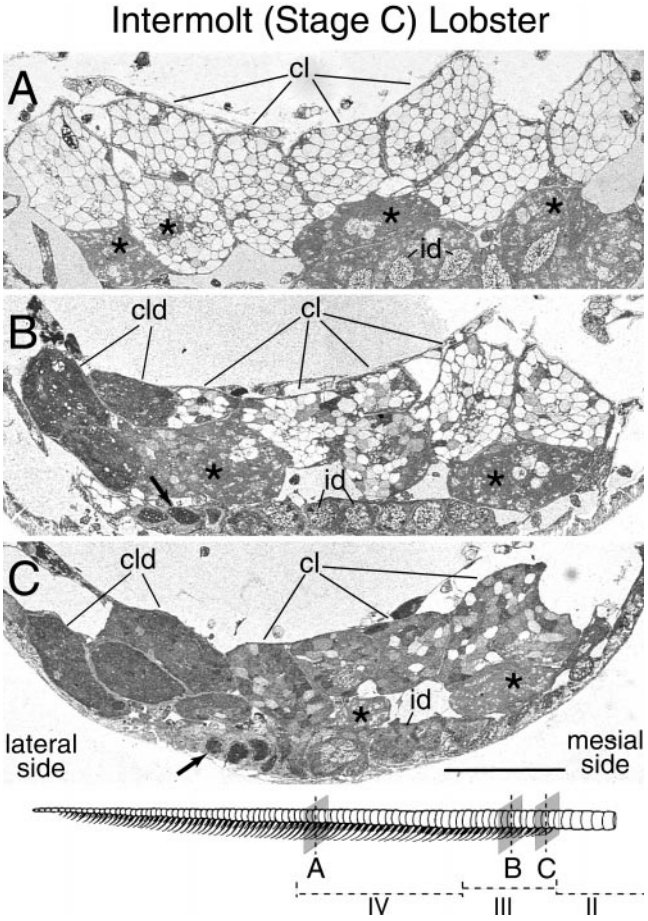

Figure 6. Taurine-like immunoreactivity in ORNs of an intermolt lobster (stage C). *Drawing, Bottom,* The aesthetasc-bearing region with the positions in the developmental zones of the transverse sections shown in *A–C*. *A*, Transverse section through clusters of ORN cell bodies (*cl*) associated with existing and mature aesthetascs in the medial part of the aesthetasc region (*zone IV*; see *drawing*). Note a lack of taurine-like IR in ORNs but a presence of taurine-like IR in the supporting cells (*). *B*, Transverse section through clusters of ORN cell bodies (*cl*) associated with newly emerged aesthetascs in a new row of sensilla located six annuli distal to the proximal end of the aesthetasc-bearing region (medial part of *zone III*; see *drawing*). *C*, Transverse section through clusters of ORN cell bodies (*cl*) associated with newly emerged aesthetascs in a new row of sensilla located one annulus distal to the proximal end of the aesthetasc-bearing region (proximal part of *zone III*; see *drawing*). In *B* and *C,* note on the *lateral side* the presence of cell body clusters (*cld*) and inner dendrites (*arrow*) of developing ORNs associated with aesthetascs that have not yet emerged at the cuticular surface but will at the next molt. Note the very high and uniform level of taurine-like IR in ORNs of these developing clusters, compared with the weaker and more variable taurine-like IR in ORNs of the newly emerged aesthetascs. Note also the greater degree of taurine-like IR in ORN clusters of emerged aesthetascs (*cl*) in *C* than in *B*. *id*, Inner dendrites of ORNs associated with a single aesthetasc; *, supporting cells. Scale bar, 100 μm.

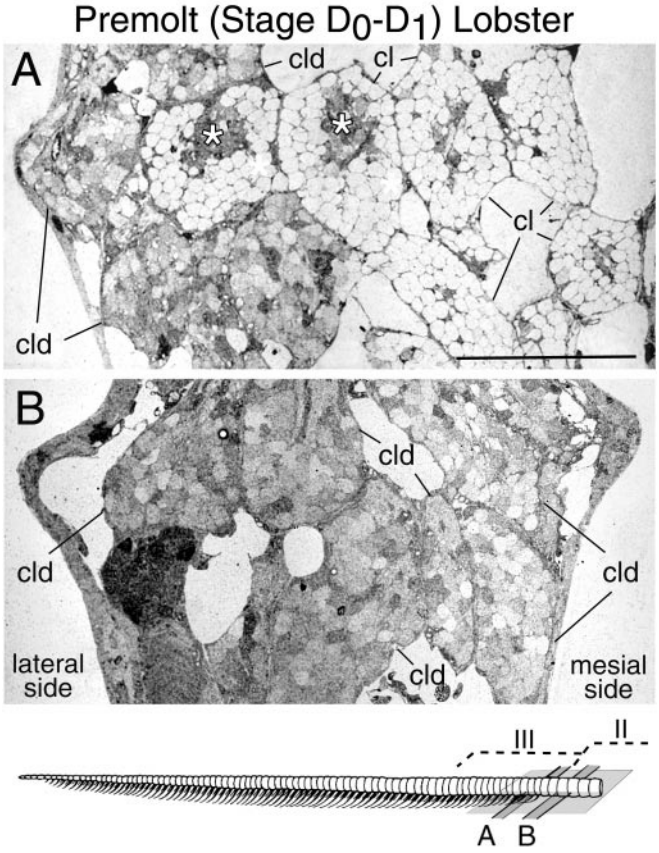

Figure 7. Taurine-like immunoreactivity in ORNs of a premolt lobster (stage D_0–D_1 or ~3 weeks before molting). *Drawing, Bottom,* The positions along the flagellum of the horizontal sections shown in *A* and *B*. *A,* Horizontal section through clusters of ORN cell bodies associated with aesthetascs in the most proximal annulus with emerged aesthetascs (proximal part of *zone III*; see *drawing*). Clusters of ORNs without taurine-like IR (*cl*) are associated with aesthetascs that emerged at the cuticular surface at the previous molt. Clusters of ORNs with taurine-like IR (*cld*) are associated with developing aesthetascs that will emerge at the cuticular surface at the next molt and are located on the lateral side of rows of emerged aesthetascs. Supporting cells (*) of the aesthetascs also show elevated taurine-like IR. *B*, Horizontal section through clusters of ORN cell bodies (*cld*) associated with developing aesthetascs in the third most distal annuli with no emerged aesthetascs (distal part of *zone II*; see *drawing*). This figure shows that the ORNs of aesthetascs ready to emerge (*cld*) on the lateral side of existing rows (in *zone III*; *A*) and in the nonaesthetasc-bearing annuli (*zone II*; *B*) had relatively lower levels of taurine-like IR than ORNs of developing aesthetascs during the intermolt stage (Fig. 6*B,C, cld*). By the end of the premolt stage (1–3 d before molting; stage D_3–D_4), most of the ORNs from the most distal developing aesthetascs (in *zone III*) that are ready to emerge did not have taurine-like IR, whereas ORNs from more proximal developing aesthetascs (in *zone II*) still showed taurine-like IR (data not shown). Scale bar, 100 μm.

a very few did not, showing a developing shaft that only partially made its way through the new cuticle.

Taurine-like immunoreactivity in ORNs

Taurine-like IR occurred in the cytoplasm of some ORNs, but its incidence depended on the age and maturity of the ORNs. In aesthetascs that were >1 molt cycle old (in zones IV–VI), ORNs typically showed no cytoplasmic taurine-like IR during the entire molt cycle (see Figs. 6*A*, 8*A*). Only a few ORNs in some clusters of some flagella contained a detectable level of taurine-like IR in these regions. This contrasted with the generally high level of taurine-like IR in the inner dendrites, cell bodies, and axons of ORNs from the developing aesthetascs in zones II and III and from most of the newly emerged aesthetascs in zone III. In zones II and III, taurine-like IR was particularly elevated in developing ORNs associated with clusters that appeared during the postmolt and intermolt stages; taurine-like IR was so high that the boundaries of individual cells were not visible (Fig. 6*B,C*). By the end of the intermolt stage and throughout the premolt stage, the levels of taurine-like IR gradually decreased (Fig. 7), eventually to reach undetectable levels by the end of the premolt stage in many

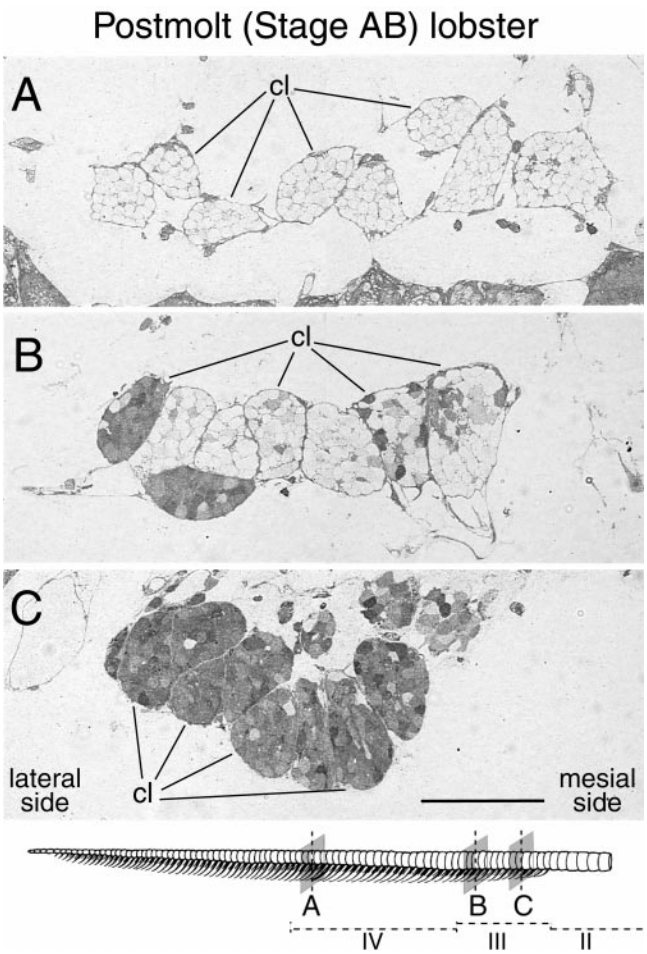

Figure 8. Taurine-like immunoreactivity in ORNs of a postmolt lobster (stage AB). *Drawing, Bottom,* The aesthetasc-bearing region with the positions in the developmental zones of the transverse sections shown in *A–C*. *A*, Transverse section through clusters of ORN cell bodies (*cl*) associated with existing and mature aesthetascs in the medial part of the aesthetasc region (*zone IV*; see *drawing*). Note a lack of taurine-like IR in ORNs. *B*, Transverse section through clusters of ORN cell bodies (*cl*) associated with newly emerged aesthetascs in a new row of sensilla located 11 annuli distal to the proximal end of the aesthetasc-bearing region (distal part of *zone III*; see *drawing*). Note that clusters located on the *lateral side* have more ORNs with high taurine-like IR than do ORNs on the *mesial side*. *C*, Transverse section through clusters of ORN cell bodies (*cl*) associated with newly emerged aesthetascs in a new row of sensilla located four annuli distal to the proximal end of the aesthetasc-bearing region (proximal part of *zone III*; see *drawing*). By contrast to *A*, note in *B* and *C* the high taurine-like IR in many ORNs. Scale bar, 100 μm.

ORNs associated with the most distal differentiating aesthetascs (in zone III), but remained elevated in ORNs of more proximal developing aesthetascs (in zone II).

After molting, the decrease in taurine-like IR continued in ORNs of the new rows of emerged aesthetascs (Fig. 8) and gradually propagated from the most mesiodistal to the most lateroproximal new aesthetascs throughout the postmolt and intermolt stages (Fig. 9). Thus the decrease in taurine-like IR occurred sooner in the most distal rows of new aesthetascs than in the most proximal rows (Fig. 9; see also Figs. 6*B* vs *C*, 8*B* vs *C*) and sooner in the mesial side of a row than in the lateral side (Fig. 9; see also Fig. 8*B*). During the postmolt stage, many ORNs from the most distal annuli with new rows of emerged aesthetascs completely lost their taurine-like IR (Fig. 9; see also Fig. 8*B*). On the other hand, ORNs from aesthetascs located on the most proximal annuli and particularly from those on the lateral side of a row retained high levels of taurine-like IR throughout the postmolt stage and most of the intermolt stage (Figs. 6*C*, 8*C*, 9). The decrease in taurine-like IR was asynchronous among ORNs of a single aesthetasc, as shown by the heterogeneity in taurine-like IR in ORNs (Figs. 6*B,C*, 7, 8*B*). Finally, complete loss of taurine-like IR was achieved in most ORNs of most new aesthetascs, including the most proximal ones, sometime during the end of the intermolt stage and the next premolt stage (Fig. 7*A*).

In summary, the decrease in taurine-like IR was not synchronous among all ORNs of new aesthetascs and was not dependent on the emergence of the sensilla at the cuticular surface. The decrease in taurine-like IR propagated gradually and continually from the most distal new aesthetascs to the most proximal and lateral ones (Fig. 10). Before molting, the absence of taurine-like IR was already observed in ORNs of the most distal developing aesthetascs in zone II, whereas taurine-like IR in ORNs of the most proximal and lateral new aesthetascs only disappeared weeks to months after the sensillar emergence at the cuticular surface.

Functional maturation of new ORNs

To examine when ORNs become functionally mature, we used an odor activity-labeling technique to compare the frequency of odor-activated ORNs in different antennular zones and thus different developmental ages. We used a technique that is based on the entry of agmatine through cation channels after odor activation. As described in Materials and Methods, this technique is an effective measure of the relative differences in the number of ORNs of different developmental ages that are excited by and best-tuned to the odorant stimulus. The results show that during intermolt and early premolt stages (C and beginning of D_0, respectively), the percentage of odor activity-labeled ORNs in old aesthetascs (>1 molt cycle old; zones IV and V) was higher than that in new aesthetascs that just emerged in zone III (Fig. 11). This was true for all flagella stimulated by any one of five single odorants (AMP, cysteine, glycine, NH_4, or proline), a complex odor mixture (oyster mixture), or even agmatine alone (control), which is a weak odor stimulant by itself (Michel et al., 1999). Figure 11 shows that the percentage of ORNs activated by either the single odorants (data pooled), the oyster mixture, or agmatine alone was significantly greater in the old than in the new aesthetascs.

In new aesthetascs, there was a statistically significant inverse correlation between the extent of taurine-like IR and the percentage of odor-responsive ORNs stimulated with single odorants (Fig. 11). A trend toward an inverse correlation between the level of taurine-like IR and the level of odor-dependent activity labeling in new aesthetascs stimulated with either the oyster mixture or agmatine alone was also observed, but the trend was nonsignificant because of the small sample size. Figure 11 shows that aesthetascs having many ORNs with taurine-like IR possessed fewer odor-activated ORNs than did aesthetascs containing no or only a few ORNs with taurine-like IR. On the basis of analysis of 408 odor-activated ORNs in new aesthetascs from 13 flagella, 396 or 97% of the odor-activated ORNs did not show taurine-like IR, whereas only 12 or 3% of the odor-activated ORNs showed taurine-like IR. For new aesthetascs with <50% of their ORNs showing taurine-like IR, <1% (1 out of 131) of their odor-activated ORNs showed taurine-like IR. For new aesthetascs with >50% of their ORNs showing taurine-like IR, only 39% (7 out of

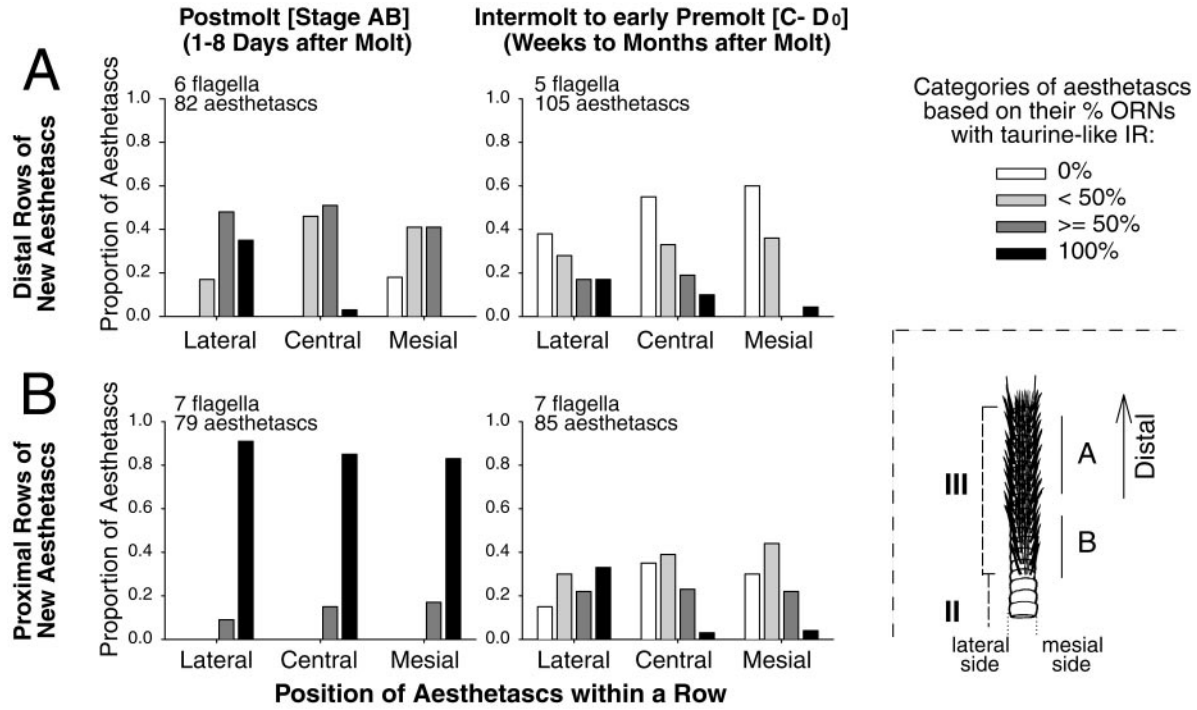

Figure 9. Taurine-like immunoreactivity in ORNs shows a spatiotemporal gradient in rows of newly emerged aesthetascs (*zone III*). Taurine-like IR in new ORNs decreases slowly but asynchronously over time after a molt, with ORNs of proximal and lateral aesthetascs retaining high levels of taurine-like IR for longer time periods than ORNs of distal and mesial aesthetascs. *A*, Distal rows of new aesthetascs that are located 9–15 annuli distal from the proximal end of the aesthetasc region (Fig. 4, region ~0 to −10; see *drawing, bottom right*). At the postmolt stage, aesthetascs have ORNs with variable levels of taurine-like IR. A small proportion of mesial aesthetascs contains ORNs without taurine-like IR, whereas a large proportion of lateral aesthetascs contains only ORNs with taurine-like IR. At the intermolt stage, a large proportion of aesthetascs has only ORNs without taurine-like IR, especially in the mesial aesthetascs. *B*, Proximal rows of new aesthetascs that are located on the six most proximal annuli of the aesthetasc region (Fig. 4, region approximately −10 to −20; see *drawing, bottom right*). At the postmolt stage, all aesthetascs have all or most of their ORNs with taurine-like IR. At the intermolt stage, an increasing proportion of aesthetascs has ORNs without taurine-like IR, especially in the mesial aesthetascs. Lateral and mesial aesthetascs are the two most lateral and mesial aesthetascs within a row, respectively.

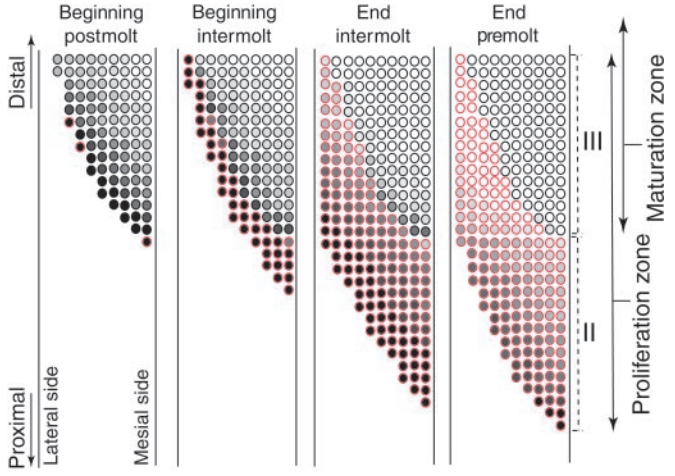

Figure 10. Schematic model of the spatiotemporal wave of differentiation and maturation of ORNs in clusters of developing aesthetascs (*circles* with *red line*) and newly emerged aesthetascs (*circles* with *black line*) throughout a molt cycle. Levels of *grays* within the *circles* indicate different levels of taurine-like IR in ORNs of a cluster; an *empty circle* symbolizes a cluster for which no ORNs have taurine-like IR. ORNs from newly emerged aesthetascs, particularly those with high taurine-like IR, are also less likely to be odor responsive (see Fig. 11). Developmental zones (Fig. 5, *II*, *III*) are given on the *right side* of the figure.

18) of the odor-activated ORNs had taurine-like IR. Moreover, when new aesthetascs had no ORNs with taurine-like IR, the percentage of odor-responsive ORNs still remained significantly lower than that in old aesthetascs (Fig. 11).

DISCUSSION

Extensive turnover of aesthetascs and their ORNs

This study demonstrates that there exists significant turnover of aesthetascs and their ORNs on the lateral flagellum of the antennules of young adult spiny lobsters. This turnover includes neurogenesis, functional maturation, and death. In the spiny lobsters examined in our study, complete turnover of the aesthetasc-bearing annuli is achieved at least after approximately six molt cycles. This turnover might be, however, faster because damage of the distal part of the aesthetasc-bearing region is quite common. Because on a given annulus addition of aesthetascs occurs over two molt cycles and gradual loss of aesthetascs spreads over at least three molt cycles, the life span of a particular aesthetasc and its ORNs might be as short as three molt cycles, or 6–12 months according to Travis (1954). Interestingly, the life span of mature ORNs in rodents is quite comparable with that in lobsters, generally varying from approximately a month to at least a year (Hinds et al., 1984; Mackay-Sim and Kittel, 1991b).

The extent of turnover described here is based on net changes in the number of aesthetascs per annulus and therefore might be an underestimation of the true turnover if replacement of aesthetascs occurs within existing rows of aesthetascs, or if turnover

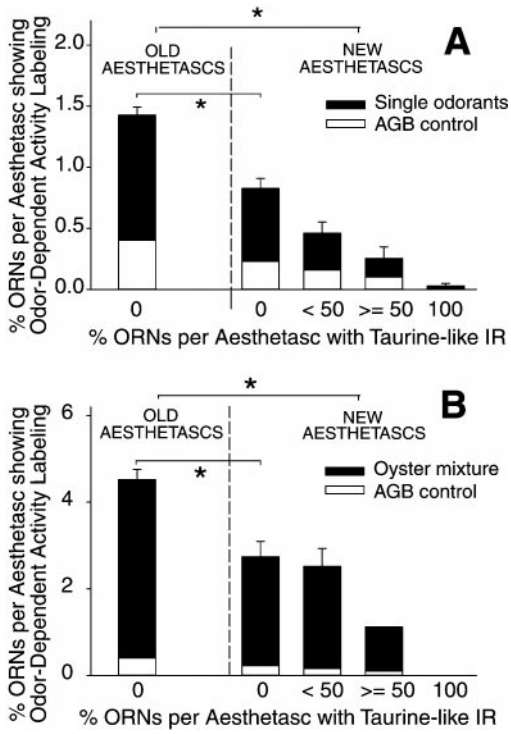

Figure 11. Odor-dependent activity labeling of ORNs in different stages of development. In lateral flagella of intermolt (stage C) and very early premolt (beginning stage D_0) lobsters, newly emerged aesthetascs contain fewer odor-dependent activity-labeled ORNs than do old aesthetascs (>1 molt cycle old), and new aesthetascs with many ORNs with elevated levels of taurine-like IR contain fewer odor-dependent activity-labeled ORNs than do new aesthetascs with no or a few ORNs with taurine-like IR. *A*, Flagella ($n = 9$) stimulated with a single odorant compound (either NH_4, AMP, glycine, proline, or cysteine) and flagella ($n = 2$) not odor stimulated [only agmatine (*AGB control*)]. All flagella stimulated with any of the single odorants showed the same trend and were pooled together. The percentage of ORNs with taurine-like IR is inversely correlated with the percentage of ORNs with odor-dependent activity labeling in flagella stimulated with single odorants ($p < 0.05$, nonparametric gamma correlation test, Statistica; StatSoft, Tulsa, OK). *B*, Flagella ($n = 3$) stimulated with the oyster mixture (a 33-component odor mixture) and flagella ($n = 2$) not odor stimulated [agmatine only (*AGB control*)]. There was a nonsignificant trend toward an inverse correlation between the percentage of ORNs with odor-dependent activity labeling and the percentage of taurine-like IR ORNs in flagella stimulated with either the oyster mixture or agmatine alone ($p > 0.05$, nonparametric gamma correlation test). *Significant difference in odor activity labeling ($p < 0.05$, Kruskal–Wallis nonparametric ANOVA).

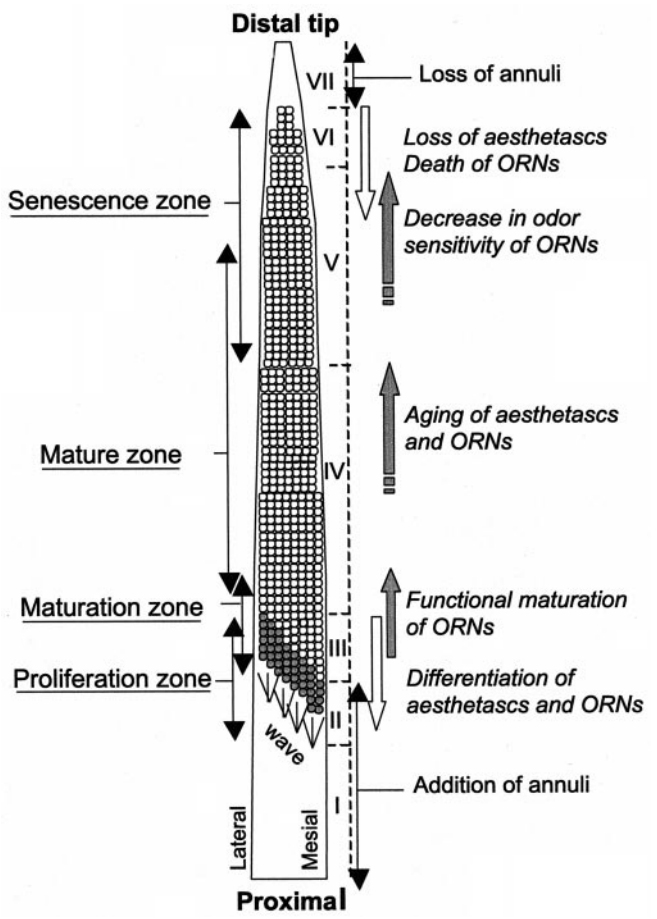

Figure 12. Schematic summary of the turnover of aesthetascs in the lateral flagellum of the spiny lobster (see Discussion). *Open circles* represent emerged aesthetascs; *dark circles* indicate developing aesthetascs that will emerge at the cuticular surface at the following molt. The developmental *zones I–VII* are described in Results and Figure 5.

of ORNs takes place within existing sensilla. The occasional presence of ORNs with taurine-like IR in aesthetascs that are >1 molt cycle old (zones IV–VI) suggests the existence of such turnover. To investigate the full extent of turnover of ORNs, our laboratory is currently using bromodeoxyuridine and TUNEL techniques to identify more directly the birth and death of ORNs along the flagellum (P. J. H. Harrison and H. S. Cate, unpublished data). However, it is likely that the general pattern of turnover that we describe here is typical.

A spatiotemporal gradient to turnover

The turnover in the spiny lobster's olfactory organ is variable in time and space. Turnover is closely related to the timing of the animal's molt cycle, in that sensilla disappear and appear at the cuticular surface of the flagellum at each molt. It is however still unclear whether the underlying determination of neuronal fate, cell division, and differentiation of the new sensilla is continuous or whether it takes place during discrete time windows within the molt cycles. The morphological immaturity of the most proximal newly emerged aesthetascs, the spatiotemporal wave of changes in taurine-like IR in ORNs of developing and newly emerged aesthetascs, and the functional maturation of ORNs in newly emerged aesthetascs suggest that the development and maturation of ORNs are continuous processes. However, whether or not the rates change over the molt cycle is currently not known. There is also a spatial separation of the birth and death of sensilla; at each molt, new aesthetascs and their ORNs appear on proximal annuli, whereas old aesthetascs are lost on distal annuli. This turnover creates a proximodistal gradient of aesthetascs of different ages; the youngest, functionally immature ones are located on the most proximal annuli, and the oldest ones that gradually lose their odor sensitivity (Steullet et al., 2000) are housed on the most distal annuli (Fig. 12). The postembryonic development of the lobster antennule with addition of annuli and sensory structures in the proximal part of the appendage and loss in the distal part is quite similar to the postembryonic development of the crayfish antennule (Sandeman and Sandeman, 1996) and the cockroach antenna (Schafer and Sanchez, 1973). This pattern of turnover is remarkably similar to the turnover of the epithelial and sensory cells on the tentacles of *Hydra* (Yaross et al., 1986; Bode, 1992).

Turnover of olfactory organs has been examined now for two species of crustaceans: *P. argus* and the crayfish *Cherax destructor* (Sandeman and Sandeman, 1996). Both species undergo a similar pattern of aesthetasc turnover, with some variations on the theme. Whereas in crayfish the most distal annuli that bear the oldest aesthetascs are shed during molting, in spiny lobsters a loss of aesthetascs usually occurs by a gradual decrease in the number of aesthetascs in the medial and distal annuli until the distalmost annuli do not bear any aesthetascs. In spiny lobsters, the most distal annuli are shed at molting and between molts, but unlike in crayfish, these distalmost annuli usually bear no aesthetascs when they are shed. In both crayfish and lobsters, growth of the antennules occurs by division of proximal annuli, and addition of aesthetascs takes place proximal to the aesthetasc-bearing region. In spiny lobsters, addition of new rows of aesthetascs can occur in dividing annuli. Such addition of annuli in the proliferation zone of new rows of aesthetascs seems to be the result of a reorganization of the antennular segmentation by the splitting of long annuli of variable length into short ones of constant length. The developing rows of aesthetascs that are forming under the cuticle at constant intervals might be implicated in this reorganization of the segmentation, so every new aesthetasc-bearing annulus will have two rows of aesthetascs.

Function and control of turnover of ORNs

The extensive turnover of ORNs might be related to the fact that spiny lobsters have long life spans. Turnover of the ORNs is well known in vertebrates (Calof et al., 1996, 1998), snails (Chase and Rieling, 1986), and crayfish (Sandeman and Sandeman, 1996), animals that can live at least 2 or more years. A long life span may have imposed physiological adaptations such as the replacement of damaged and old sensory neurons. Dendrites that are the sites of odor detection innervate the shaft of the permeable sensilla and therefore are exposed to environmental hazards, toxic chemicals, microbes, and physical damage. The addition of new ORNs in crayfish is correlated with the neurogenesis of olfactory interneurons in the olfactory lobes (Sandeman et al., 1998; Schmidt and Harzsch, 1999). Such addition of interneurons probably functions to process the additional sensory input.

What controls the death and birth of aesthetascs and their ORNs in lobsters is unknown. The life span of the sensory and supporting cells associated with aesthetascs might be genetically determined and their death programmed. But other factors might be involved in cell death. Mechanical damage of the lateral flagellum is quite common. The supply of nutrients and oxygen to the tip of these thin and long antennules might eventually become deficient, inducing a loss of sensilla and a dramatic shrinkage of the distalmost annuli. This idea is supported by our observation that the two longest premolt flagella that we examined lost ~300 aesthetascs during a molt, whereas most other flagella had a slight overall net increase in the number of aesthetascs. The balance between loss and addition of sensilla might vary with the size and age of the animal. In crayfish, animals of all sizes and ages add aesthetascs, but only larger and older ones lose aesthetascs (Sandeman and Sandeman, 1996). Furthermore in our study, the flagellum that gained the most new aesthetascs at molting had been broken off in the medial part of its aesthetasc-bearing region before the molt. Thus, the proliferation of new aesthetascs and their ORNs may be upregulated by the damage and death of sensory neurons, as has been described in the vertebrate olfactory epithelium (Calof et al., 1998) and the retina of fish and amphibians (Reh and Levine, 1998).

The spatiotemporal spread of the differentiation of sensilla that starts in the more proximal aesthetasc-bearing annuli and propagates proximally in the nonaesthetasc-bearing annuli (Figs. 10, 12) suggests that initiation of aesthetasc differentiation depends on the presence of existing aesthetascs in the close distal vicinity. Thus, cell–cell contact and/or diffusible cues emanating from the developing and newly developed aesthetascs might be essential to initiate sensillar formation in the next proximal annuli. Spatiotemporal waves of differentiation occur during development of fly sense organs with high spatial organization, including labellar bristles (Ray et al., 1993; Ray and Rodrigues, 1994), taste sensilla (Pollack and Lakes-Harlan, 1995; Pollack and Balakrishnan, 1997), olfactory sensilla (Reddy et al., 1997), mechanosensory sensilla (Hartenstein, 1988; Hartenstein and Posakony, 1989), and ommatidia (Banerjee and Zipursky, 1990; Brown et al., 1995). Thus, the development of earlier neural structures may provide cues for the elaboration of the pattern of the later ones, and the temporal interspersing of cell division and differentiation may allow correct positioning of the sensory structures (Ray and Rodrigues, 1994).

The stereotyped organization of aesthetascs and their neighboring sensilla suggests that differentiation of all these sensilla may be under the control of related factors and that differentiation of all sensillar types is interdependent. Guard hairs often emerged at the cuticular surface on one or a few annuli proximal to the aesthetasc-bearing region. It can be hypothesized that guard hairs might differentiate before aesthetascs and therefore might be involved in the initiation of aesthetasc differentiation. Additionally, some annuli lack the asymmetric and the lateral companion hairs but instead have a different pair of setae: a long lateral seta and a plumose seta (Figs. 1*D,E*, 2). This suggests the existence of regulatory factors that switch the development from one sensillar type to another, as is known in the antenna of *Drosophila* (Dambly-Chaudière et al., 1992).

Taurine-like immunoreactivity reveals developing ORNs

Our results show that ORNs of mature aesthetascs typically lack taurine-like IR throughout the lobster's molt cycle. However, taurine-like IR is elevated in developing ORNs, gradually decreases, and eventually vanishes first in ORNs of the most distal developing aesthetascs before their emergence and at last in ORNs of the most proximal and lateral aesthetascs by the premolt stage after sensillar emergence. This strongly suggests that taurine-like IR reveals a developmental stage of the aesthetasc ORNs. Heterogeneity in taurine-like IR within ORNs of single newly emerged aesthetascs also indicates differences in the developmental stage of ORNs within a sensillum.

Taurine is abundant in the brain of invertebrates (Evans, 1973; Meyer et al., 1980; Holman and Cook, 1982; Schäfer et al., 1988; Picones et al., 1992) and vertebrates (Sturman, 1993), especially in brain and sensory neurons during metamorphosis of holometabolous insects (Bodnaryk, 1981; Eichmüller and Schäfer, 1995) and in brains of newborn and young mammals (Sturman, 1993). Although taurine is prevalent in developing nervous systems, there are few definitive answers and unifying themes about its mechanism of action. There is evidence that taurine causes proliferation and/or differentiation of receptor neurons in the vertebrate visual (Altschuler et al., 1993) and olfactory (Kratzkin et al., 1999) systems. Taurine promotes cell migration (Morán et al., 1996) and protection against excitotoxicity (El Idrissi and Trenkner, 1999) in developing cerebellar granule cells, optimal neurite outgrowth, and synapse formation in the cerebellum, hippocampus, and

neocortex (Magnusson, 1996; Flint et al., 1998). A deficiency in taurine induces degeneration of the developing retina and malformations of the brain in postnatal rats and cats (Sturman, 1993). All together, these studies suggest that taurine is an important compound during the development of neurons and is involved in neuron differentiation, survival, neurite outgrowth, and synapse formation. However, the specific function of taurine during the development of aesthetasc ORNs is unknown.

Slow and gradual maturation of new ORNs

Maturation of ORNs in new aesthetascs is slow and asynchronous. Based on taurine-like IR and the fact that odor responsiveness is inversely correlated with the level of taurine-like IR, the spatiotemporal wave of ORN maturation propagates along a distoproximal and mesiolateral axis and presumably reflects the existence of a preceding wave of aesthetasc differentiation similar to that illustrated in Figure 10. Thus, ORNs belonging to the first aesthetascs to differentiate are the first to mature functionally after the molt. The fact that ORN maturation occurs throughout the molt cycle in lobsters strongly contrasts with the tight synchronization of ORN maturation with molting in insects undergoing metamorphosis (Hildebrand, 1982; Masson and Arnold, 1984; Dickens and Moorman, 1990). Throughout the intermolt stage in lobsters, the number of odor-responsive ORNs remains significantly lower in newly emerged aesthetascs than in older ones. Because the intermolt stage in the spiny lobsters of the size examined lasts 2–8 months depending on the season (Travis, 1954), this indicates a very slow functional maturation of aesthetasc ORNs. Such slow maturation contrasts with the maturation of ORNs in other arthropods and vertebrates, and their rate of maturation may be related to the timing of their synapse formation with their central targets. Odor responsiveness often coincides with or follows the establishment of mature synapses between ORNs and interneurons in mammal embryos (Gesteland et al., 1982; Farbman, 1992; Menco et al., 1994) and in insects (Hildebrand, 1982; Masson and Arnold, 1984; Devaud and Masson, 1999). In adult rats, most of the developing ORNs are dying after 2–4 weeks, suggesting a failure to make proper connections in the olfactory bulb within this critical period (Hinds et al., 1984; Mackay-Sim and Kittel, 1991a). The formation of synapses onto proper targets appears to be a determinant factor for the final maturation and survival of neurons (Oppenheim, 1991). At an average axonal growth rate of 1–3 mm/d, which is similar to estimates for olfactory receptor neurons in larval *Manduca sexta* (L. P. Tolbert, personal communication) and garfish (Cancalon, 1987) and mechanoreceptor neurons in the cerci of crickets (W. W. Walthall, personal communication), completion of the process of axonal outgrowth and formation of synapses on the appropriate targets might take 1–5 months in young adult spiny lobsters, given that a distance of 10–15 cm separates the ORN proliferation zone from the central synaptic targets of the ORNs. This corresponds approximately to the average duration of a molt cycle in these lobsters. Thus, high levels of taurine-like IR in new ORNs of intermolt lobsters might reflect an incomplete maturation because of the absence of functional synapses. However, new aesthetascs with all ORNs lacking detectable taurine-like IR still possess significantly fewer odor-sensitive ORNs than do old aesthetascs. This also suggests that elements of the olfactory transduction cascade might not be fully expressed in new ORNs, even after a decrease of taurine to undetectable levels.

REFERENCES

Altschuler D, Lo-Turco JJ, Rush J, Cepko C (1993) Taurine promotes the differentiation of a vertebrate retinal cell type *in vitro*. Development 119:1317–1328.

Banerjee U, Zipursky SL (1990) The role of cell-cell interaction in the development of the *Drosophila* visual system. Neuron 4:177–187.

Bode HR (1992) Neuron determination in the ever-changing nervous system of *Hydra*. In: Determinants of neuronal identity (Shankland M, Macagno ER, eds), pp 323–357. New York: Academic.

Bodnaryk RP (1981) Developmental changes in brain taurine levels during metamorphosis of the moth, *Mamestra configurata*. WLK Insect Biochem 11:9–16.

Brézot P, Tauban D, Renou M (1997) Sense organs on the antennal flagellum of the green stink bug, *Nezara viridula* (L.) (Heteroptera: Pentatomidae): sensillum types and numerical growth during the postembryonic development. Int J Insect Morphol Embryol 25:427–441.

Brown NL, Sattler CA, Paddock SW, Carroll SB (1995) Hairy and Emc negatively regulate morphogenetic furrow progression in the *Drosophila* eye. Cell 80:879–887.

Calof AL, Hagiwara N, Holcomb JD, Mumm JS, Shou J (1996) Neurogenesis and cell death in olfactory epithelium. J Neurobiol 30:67–81.

Calof AL, Mumm JS, Rim PC, Shou J (1998) The neuronal stem cell of the olfactory epithelium. J Neurobiol 36:190–205.

Cancalon PF (1987) Survival and subsequent regeneration of olfactory neurons after a distal axonal lesion. J Neurocytol 16:829–841.

Carr WES (1988) The molecular nature of chemical stimuli in the aquatic environment. In: Sensory biology of aquatic animals (Atema J, Fay RR, Popper AN, Tavolga WN, eds), pp 3–27. New York: Springer.

Carr WES, Derby CD (1986) Chemically stimulated feeding behavior in marine animals: importance of chemical mixtures and involvement of mixture interactions. J Chem Ecol 12:989–1011.

Chapman RF, Greenwood M (1986) Changes in distribution and abundance of antennal sensilla during growth of *Locusta migratoria* L. (Orthoptera: Acrididae). Int J Insect Morphol Embryol 15:83–96.

Chase R, Rieling R (1986) Autoradiographic evidence for receptor cell renewal in the olfactory epithelium of a snail. Brain Res 384:232–239.

Dambly-Chaudière C, Jamet E, Burri M, Bopp D, Basler K, Hafen E, Dumont N, Spielman P, Ghysen A, Noll M (1992) The paired box gene pox neuro: a determinant of poly-innervated sense organs in *Drosophila*. Cell 69:159–172.

Derby CD (1995) Single unit electrophysiological recording techniques from crustacean chemoreceptor neurons. In: CRC handbook on experimental cell biology of taste and olfaction: current techniques and protocols (Spielman AI, Brand JD, eds), pp 241–250. Boca Raton, FL: CRC.

Derby CD (2000) Learning from spiny lobsters about chemosensory coding of mixtures. Physiol Behav, in press.

Devaud JM, Masson C (1999) Dendritic pattern of development of the honeybee antennal lobe neurons: a laser scanning confocal microscopic study. J Neurobiol 39:461–474.

Dickens JC, Moorman EE (1990) Maturation and maintenance of electroantennogram responses to pheromone and host odors in boll weevils *Anthonomus grandis* Boh. (Col., Curculionidae) fed their host plant or an artificial diet. J Appl Entomol 109:470–480.

Eichmüller S, Schäfer S (1995) Sensory neuron development revealed by taurine-immunocytochemistry in the honeybee. J Comp Neurol 352:297–397.

El Idrissi A, Trenkner E (1999) Growth factors and taurine protect against excitotoxicity by stabilizing calcium homeostasis and energy metabolism. J Neurosci 19:9454–9468.

Evans PD (1973) Amino acid distribution in the nervous system of the crab, *Carcinus maenas* (L.). J Neurochem 21:11–17.

Farbman AI (1992) Cell biology of olfaction. Cambridge, UK: Cambridge UP.

Flint AC, Xiaolin Liu, Kriegstein AR (1998) Nonsynaptic glycine receptor activation during early neocortical development. Neuron 20:43–53.

Gesteland RC, Yancey RA, Farbman AI (1982) Development of olfactory receptor neuron selectivity in the rat fetus. Neuroscience 7:3127–3136.

Gleeson RA, Carr WES, Trapido-Rosenthal HG (1993) Morphological characteristics facilitating stimulus access and removal in the olfactory organ of the spiny lobster, *Panulirus argus*: insight from the design. Chem Senses 18:67–75.

Grünert U, Ache BW (1988) Ultrastructure of the aesthetasc (olfactory) sensilla of the spiny lobster *Panulirus argus*. Cell Tissue Res 251:95–103.

Hartenstein V (1988) Development of *Drosophila* larval sensory organs:

spatiotemporal pattern of sensory neurones, peripheral axonal pathways and sensilla differentiation. Development 102:869–886.
Hartenstein V, Posakony JW (1989) Development of adult sensilla on the wing and notum of *Drosophila melanogaster*. Development 107:389–405.
Hartnoll RG (1982) Growth. In: The biology of crustacea, Vol 2 (Abele LG, ed), pp 111–195. New York: Academic.
Hess E, Vlimant M (1986) Leg sense organs of ticks. In: Morphology, physiology, and behavioural biology of ticks (Sauer JR, Hair JA, eds), pp 361–390. Chichester, UK: Horwood.
Hildebrand JG (1982) Metamorphosis of the insect nervous system. Influences of the periphery on the post-embryonic development of the antennal sensory pathway in the brain of *Manduca sexta*. In: Model neural networks and behavior (Selverston AI, ed), pp 129–148. New York: Plenum.
Hinds JW, Hinds PL, McNelly NA (1984) An autoradiographic study of the mouse olfactory epithelium: evidence for long-lived receptors. Anat Rec 210:375–383.
Holman GM, Cook BJ (1982) Physiological amino acids of the nervous system of the stable fly, *Stomoxys calcitrans*. Comp Biochem Physiol A 71:23–27.
Huxtable RJ (1992) Physiological actions of taurine. Physiol Rev 72:101–163.
Jander U, Jander R (1994) Numerical allometric growth of the ommatidia, antennal sensilla, and teeth of foretibial combs in the milkweed bug *Oncopeltus fasciatus* Dallas (Heteroptera: Lygaeidae). Int J Insect Morphol Embryol 23:329–344.
Keil TA (1992) Fine structure of a developing insect olfactory organ: morphogenesis of the silkmoth antenna. Microsc Res Tech 22:351–371.
Kratzkin I, Belluzzi O, Smutzer G, Ross D, Hastings L (1999) Possible functions of taurine in the primary olfactory pathway. Chem Senses 24:532.
Lavalli KL, Factor JR (1995) The feeding appendages. In: Biology of the lobster *Homarus americanus* (Factor JR, ed), pp 349–394. London: Academic.
Laverack MS (1964) The antennular sense organs of *Panulirus argus*. Comp Biochem Physiol 13:301–321.
Lyle WG, MacDonald GD (1983) Molt stage determination in the Hawaiian spiny lobster *Panulirus marginatus*. J Crust Biol 3:208–216.
Mackay-Sim A, Kittel P (1991a) Cell dynamics in the adult mouse olfactory epithelium: a quantitative autoradiographic study. J Neurosci 11:979–984.
Mackay-Sim A, Kittel P (1991b) On the life span of olfactory receptor neurons. Eur J Neurosci 3:209–215.
Magnusson KR (1996) Distributions of taurine, glutamate, and glutamate receptors during post-natal development and plasticity in the rat brain. In: Taurine 2 (Huxtable RJ et al., eds), pp 435–444. New York: Plenum.
Marc RE (1999a) Mapping glutamatergic drive in the vertebrate retina with a channel permeant organic channel. J Comp Neurol 407:47–64.
Marc RE (1999b) Kainate activation of horizontal, bipolar, amacrine and ganglion cells in the rabbit retina. J Comp Neurol 407:65–76.
Masson C, Arnold G (1984) Ontogeny, maturation and plasticity of the olfactory system in the workerbee. J Insect Physiol 30:7–14.
Mellon Jr D, Alones V (1993) Cellular organization and growth-related plasticity of the crayfish olfactory midbrain. Microsc Res Tech 24:231–259.
Menco BPM, Tekula FD, Farbman AI, Danho W (1994) Developmental expression of G-proteins and adenylyl cyclase in peripheral olfactory systems. Light microscopic and freeze-substitution electron microscopic immunocytochemistry. J Neurocytol 23:708–727.
Meyer W, Poehling HM, Neuhoff V (1980) Comparative aspects of free amino acids in the central nervous system of spiders. Comp Biochem Physiol C 67:83–86.
Michel WC, Steullet P, Cate HS, Burns CJ, Zhainazarov AB, Derby CD (1999) High-resolution functional labeling of vertebrate and invertebrate olfactory receptor neurons using agmatine, a channel-permeant cation. J Neurosci Methods 90:143–156.
Morán J, Maar T, Gegelashvili G, Bock E, Schousboe A, Pasantes-Morales H (1996) Taurine deficiency and neuronal migration. In: Taurine 2 (Huxtable RJ et al., eds), pp 519–526. New York: Plenum.
Oppenheim RW (1991) Cell death during development of the nervous system. Annu Rev Neurosci 14:453–501.
Perry TL, Hansen S (1973) Quantification of free amino compounds of rat brain: identification of hypotaurine. J Neurochem 21:1009–1011.
Picones A, Escalera RL, Pasantes-Morales H (1992) Distribution of taurine and other free amino acids in the visual pathway of the crayfish *Procambarus clarkii*. Comp Biochem Physiol B 101:627–631.
Pollack GS, Balakrishnan R (1997) Taste sensilla of flies: function, central neuronal projections, and development. Microsc Res Tech 39:532–546.
Pollack GS, Lakes-Harlan R (1995) Birth times of neurons in labellar taste sensilla of the blowfly *Phormia regina*. J Neurobiol 26:17–32.
Ray K, Rodrigues V (1994) The function of the proneural genes *achaete* and *scute* in the spatio-temporal patterning of the adult labellar bristles of *Drosophila melanogaster*. Roux's Arch Dev Biol 203:340–350.
Ray K, Hartenstein V, Rodrigues V (1993) Development of the taste bristles on the labellum of *Drosophila melanogaster*. Dev Biol 155:26–37.
Reddy GV, Gupta B, Ray K, Rodrigues V (1997) Development of the *Drosophila* olfactory sense organs utilizes cell-cell interactions as well as lineage. Development 124:703–712.
Reh TA, Levine EM (1998) Multipotential stem cells and progenitors in the vertebrate retina. J Neurobiol 36:206–220.
Riesgo-Escovar J, Woodard C, Gaines P, Carlson J (1992) Development and organization of the *Drosophila* olfactory system: an analysis using enhancer traps. J Neurobiol 23:947–964.
Sandeman R, Clarke D, Sandeman D, Manly M (1998) Growth-related and antennular amputation-induced changes in the olfactory centers of crayfish brain. J Neurosci 18:6195–6206.
Sandeman RE, Sandeman DC (1996) Pre-embryonic and postembryonic development, growth and turnover of olfactory receptor neurons in crayfish antennules. J Exp Biol 199:2409–2418.
Schafer R, Sanchez TV (1973) Antennal sensory system of the cockroach, *Periplaneta americana*: postembyonic development and morphology of the sense organs. J Comp Neurol 149:335–354.
Schäfer S, Bickel G, Ottersen OP, Storm-Mathisen J (1988) Taurine-like immunoreactivity in the brain of the honeybee. J Comp Neurol 268:60–70.
Schmidt M, Harzsch S (1999) Comparative analysis of neurogenesis in the central olfactory pathway of adult decapod crustaceans by *in vivo* BrdU labeling. Biol Bull 196:127–136.
Skinner DM (1985) Molting and regeneration. In: The biology of crustacea, Vol 9 (Bliss DE, Mandel LH, eds), pp 43–145. New York: Academic.
Spencer M, Linberg KA (1986) Ultrastructure of aesthetasc innervation and external morphology of the lateral antennule setae of the spiny lobster *Panulirus interruptus* (Randall). Cell Tissue Res 245:69–80.
Steullet P, Cate HS, Michel WC, Derby CD (2000) Functional units of a compound nose: aesthetasc sensilla house similar populations of olfactory receptor neurons on the crustacean antennule. J Comp Neurol 418:270–280.
Sturman JA (1993) Taurine in development. Physiol Rev 73:119–147.
Travis DF (1954) The molting cycle of the spiny lobster, *Panulirus argus* Latreille. I. Molting and growth in laboratory-maintained individuals. Biol Bull 107:433–450.
Truman JW, Taylor BJ, Awad TA (1993) Formation of the adult nervous system. In: The development of *Drosophila melanogaster* (Bate M, Martinez Arias A, eds), pp 1245–1275. Cold Spring Harbor, NY: Cold Spring Harbor.
Watling L (1989) A classification system for crustacean setae based on the homology concept. In: Crustacea issues, Vol 6, Functional morphology of feeding and grooming in crustacea (Felgenhauer B, Watling L, Thistle AB, eds), pp 15–26. Rotterdam, The Netherlands: Balkema.
Yaross MS, Westerfield J, Javois LC, Bode HR (1986) Nerve cells in *Hydra*: monoclonal antibodies identify two lineages with distinct mechanisms for their incorporation into head tissue. Dev Biol 114:225–237.